Progress In Electromagnetics Research Letters, Vol. 78, 1–7, 2018

Broadband Low-Profile Circularly Polarized Antenna with Stepped Sequential Feeding Structure

Huidong Li*, Xiaoyu Du, Zhaohui Wei, Zhao Zhou, and Yingzeng Yin

Abstract—A broadband low-profile circularly polarized (CP) antenna with a stepped sequential feeding structure is proposed in this letter. The CP antenna consists of four dipoles and parasitic structures. A novel feeding network using parallel transmission lines is introduced to realize phase difference required for circular polarization. Four dipoles are excited by the feeding structure to achieve CP radiation, and parasitic elements are loaded to broaden 3-dB axial ratio bandwidth (ARBW). To verify this design, the proposed antenna is fabricated and measured. Measured results show that a 10-dB impendence bandwidth of 42% (1.82 to 2.8 GHz) and 3-dB ARBW of 36.4% (1.89 to 2.73 GHz) are achieved, respectively. Moreover, the designed antenna has a low profile of 0.13λ (λ is the free-space wavelength at the center frequency) and a gain of average 9.5 dBi with less than 1.5-dB variation within the 3-dB ARBW.

1. INTRODUCTION

With the rapid development of communication technology, the demand for communication devices is also increasing. Circularly polarized antennas have attracted more and more attention for the features of overcoming polarization mismatch effects. Besides, the antennas for some applications, such as Wi-Fi access points [1] and satellite system [2], require wide impendence bandwidth and 3-dB axial-ratio bandwidth. A common method to realize circular polarization is truncating patch corners or cutting diagonal slots in the patch. Unfortunately, these antennas only achieve a narrow 3-dB ARBW. A single-fed microstrip patch antenna with corners cut is excited with a circular disc in [3]. AR bandwidth is enhanced by employing four parasitic strips to introduce a new minimum AR, and the ARBW is improved from 8.43% to 24% in this method. Furthermore, one 3×3 and one 5×5 antenna arrays are studied in [4]. A probe-fed circularly polarized (CP) microstrip patch antenna is placed at the center as the driven antenna and is gapped coupled to the remaining elements. As a result, the 3×3 array has a measured 3 dB axial ratio bandwidth of 3.3%, and the 5×5 array has a measured 3 dB axial ratio bandwidth of 8.1%. A single-fed broadband circularly polarized stacked patch antenna is proposed in [5]. Meanwhile, some other broadband CP antennas are designed in [6–10], but there are application restrictions because none of them produce directional radiation.

Several feeding structures have been reported to realize sequential phase and power divisions. A CP loop that provides sequential phase is used in [11]. The square loop feeding structure is formed by etching a square from a smaller square to achieve stable phase rotation. An arc-shaped strip with angle of 270° is employed to feed the square loop. Besides, a sequential phase feed using uniform transmission lines is proposed in [12]. The presented SP feed in [12] employs a single stage transition where the transmission line width is uniform. However, it is difficult for structures mentioned in [11, 12] to excite dipoles with a balanced feeding. Nowadays, a stepped sequential feeding structure using integrated parallel transmission lines is presented in this letter. Four dipoles can be directly connected

Received 24 June 2018, Accepted 1 August 2018, Scheduled 11 August 2018

* Corresponding author: Huidong Li (lihuidong8090@163.com).

The authors are with the National Key Laboratory of Antennas and Microwave Technology, Xidian University, Xi'an, Shaanxi 710071, People's Republic of China.

to the feeding structure without balun. In addition, due to the high profile of traditional CP antennas, there are some limitations in application. In order to realize low-profile circularly polarized antennas, metamaterials are widely used in antenna designs [13–15]. In addition, a new kind of double layers artificial magnetic conductor (AMC) unit is applied in antenna design [16] to broaden its reflection phase bandwidth.

In this letter, a CP antenna with mirror symmetrical structure is discussed. It consists of four dipoles and a novel feeding structure that realizes sequential phase and power division. An AMC reflector is applied to reduce profile of the antenna. By optimizing parameters, a wideband CP antenna is achieved. This letter is organized as follows. Some methods about how to extend ARBW of CP antennas and realization of sequential phase are introduced in Section 1. The geometry and design of the proposed antenna are discussed in Section 2. Measured results are shown in Section 3. The conclusion is obtained in Section 4.

2. ANTENNA GEOMETRY AND DESIGN

2.1. Antenna Geometry

Figure 1 shows the geometry of the proposed CP antenna which comprises a radiator and an AMC reflector. The radiator, which is located at a height of $h0$ above the AMC plane, contains a stepped sequential feeding structure, dipoles and parasitic structures. The feeding structure is composed of integrated parallel transmission lines and printed on both sides of an FR4 substrate with a dielectric

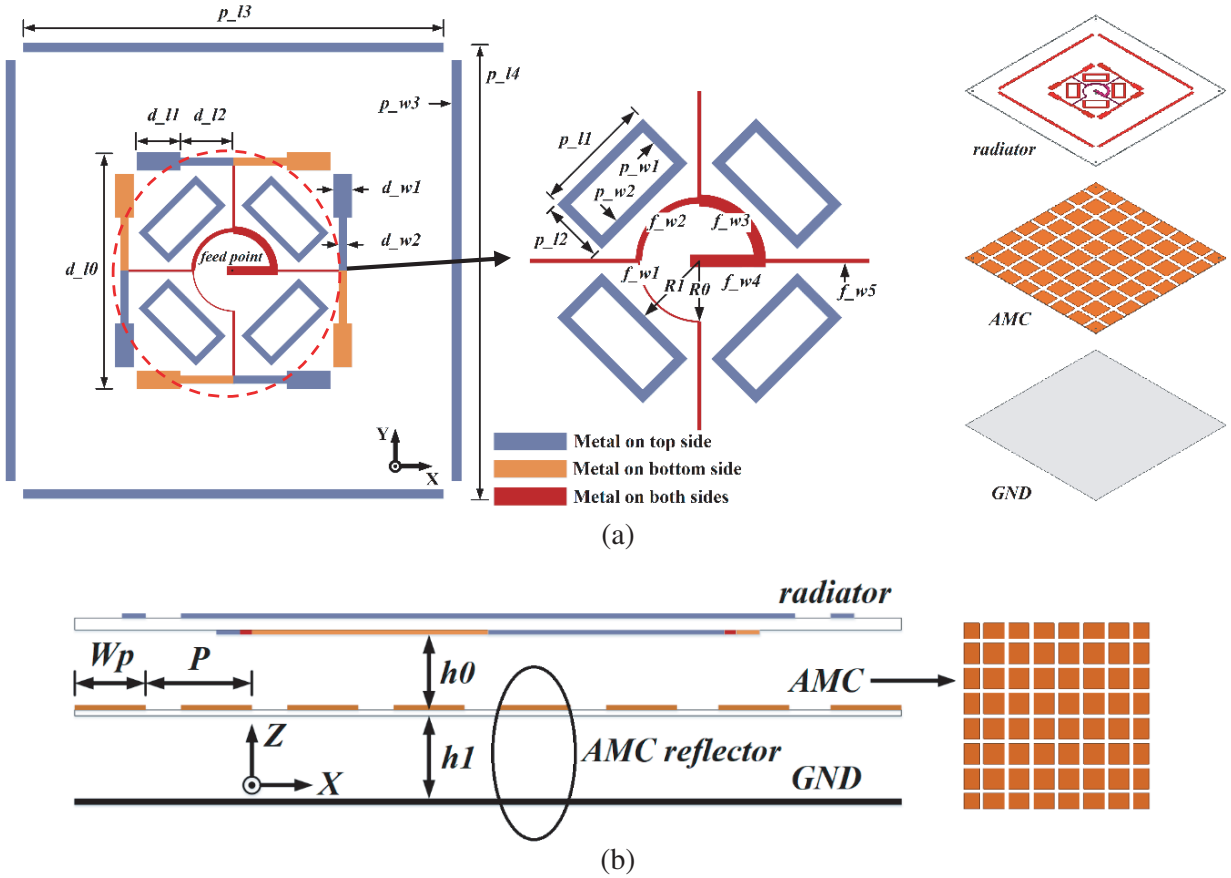

Figure 1. Geometry of the proposed antenna. Dipoles, feeding net and parasitic elements are all printed on the top substrate. AMC is printed on the lower substrate. (a) Top view of radiator and schematic diagram of the antenna, (b) side view of the proposed antenna.

constant of 4.4, loss tangent of 0.02, and thickness of 1 mm. At the feed point, inner conductor of the coaxial line is connected to the upper parallel transmission lines, and outer conductor is connected to the lower parallel transmission lines. Arms of dipoles are directly connected to parallel transmission lines to realize balanced feed. It can be seen from Fig. 1 that four parasitic rings are sequentially rotated around the feeding structure to broaden 3-dB ARBW. Meanwhile, four parasitic strips with sizes of $p\_l3 \times p\_w3$ are loaded around the dipoles to get an enhanced 3-dB ARBW. AMC is printed on the other FR4 substrate with a thickness of 0.6 mm, and the size of the square unit is $Wp \times Wp$. The designed antenna parameters are selected as follows: $h0 = 4$ mm, $h1 = 11.5$ mm, $Wp = 20$ mm, $P = 24.3$ mm, $sub\_l = 180$ mm, $d\_l0 = 73.2$ mm, $d\_l1 = 13.5$ mm, $d\_l2 = 16.4$ mm, $d\_w1 = 5.7$ mm, $d\_w2 = 2.5$ mm, $p\_l1 = 25$ mm, $p\_l2 = 13$ mm, $p\_l3 = 130$ mm, $p\_l4 = 141$ mm, $p\_w1 = 2$ mm, $p\_w2 = 2$ mm, $p\_w3 = 3$ mm, $R0 = 12.5$ mm, $R1 = 16$ mm, $f\_w1 = 0.4$ mm, $f\_w2 = 1.3$ mm, $f\_w3 = 2.4$ mm, $f\_w4 = 2.6$ mm, $f\_w5 = 0.2$ mm.

2.2. Antenna Design Process

The evolution of the antenna is shown in Fig. 2. Circularly polarized wave is obtained by two pairs of dipoles which are excited by sources with equal power and phase difference of 90°. Parasitic rings and strips are introduced to extend the 3-dB AR bandwidth. Firstly, a radiator is placed above a PEC reflector at a distance of quarter space wavelength at center frequency. As we all know, a PEC reflector provides a 180° reflection phase. In addition, wave path between radiator and PEC reflector can also achieve a 180° phase. Therefore, directionality of the antenna is strengthened due to the collective effect of reflection phase difference and wave path difference. At last, the PEC reflector is replaced by an AMC reflector for the feature of in-phase reflection.

In order to more clearly explain the effects of parasitic elements and AMC reflector, four prototypes are simulated, and Fig. 3 shows their simulated reflection coefficients and ARs in the boresight direction

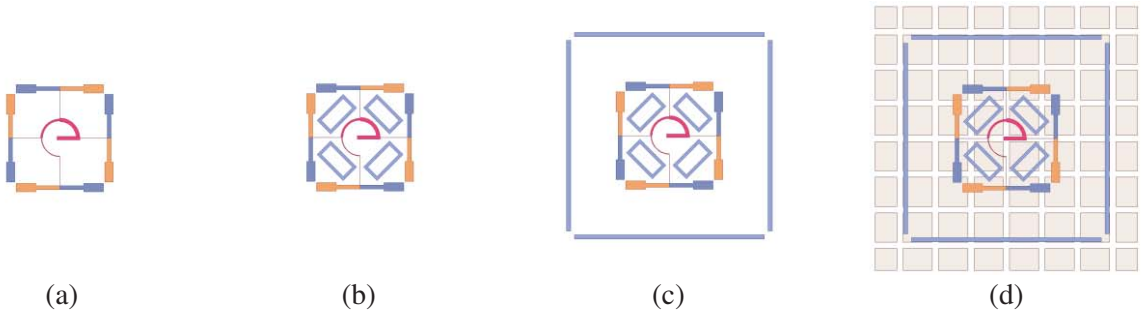

Figure 2. The evolution of the proposed antenna: (a) Antenna 1; (b) Antenna 2; (c) Antenna 3; (d) Antenna 4.

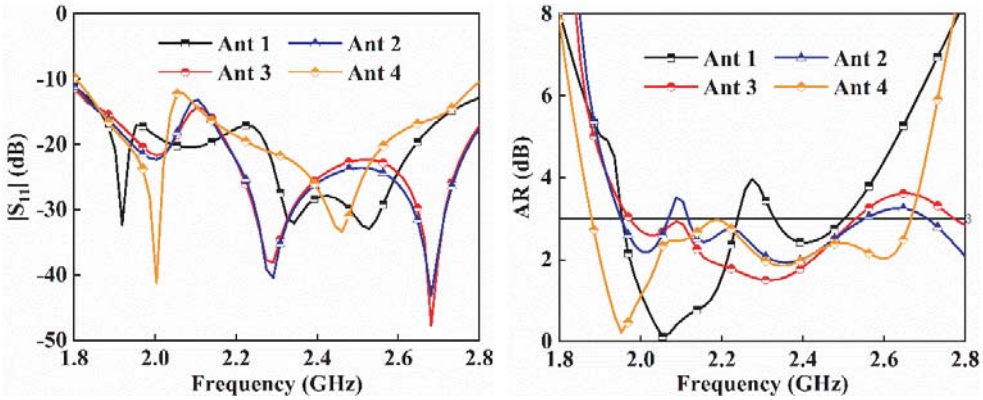

Figure 3. Simulated $|S_{11}|$ and AR of four prototypes.

($\theta = 0°$). It can be seen from Fig. 3 that the 3-dB ARBW of the traditional design using four dipoles is about 25% (Ant. 1). The introduction of parasitic rings enhances AR bandwidth significantly. Two additional AR minimums are obtained in the higher band, extending the 3-dB AR bandwidth (Ant. 2). Ant. 3 fabricates four parasitic strips around the dipoles, and this approach drops the AR curve entirely. The employment of AMC achieves a desired AR bandwidth from 1.89 to 2.73 GHz and a low profile of 0.13λ (Ant. 4). To investigate the generation of the low AR point and high AR point, we examine the current distributions on the parasitic strips and loops with a period at 2.0 and 2.6 GHz, shown in Fig. 4. It can be seen from Fig. 3 that in the lower frequency 2.0 GHz, most of the currents concentrate on two dipoles and two strips at $t = 0$. The equivalent current direction is along phi $= -90°$. Meanwhile, the currents concentrate on the other two dipoles and two strips, and the direction is along phi $= 0°$ while $t = T/4$. At the higher frequency 2.6 GHz, currents concentrate on dipoles and loops, and the equivalent current direction is along phi $= -135°$ at $t = 0$ and phi $= -45°$ at $t = T/4$. Therefore, the currents rotate counterclockwise to realize RHCP waves in the boresight direction. In addition, use of AMC drops the AR curve as a whole. The occurrence of drop of AR curve can be attributed to the fact that the surface waves propagating on the AMC structure take into effect [12].

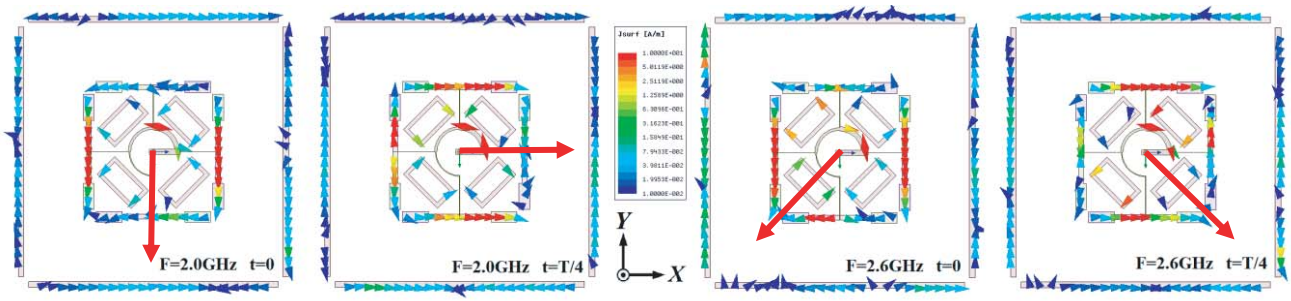

Figure 4. Current distributions on the dipoles and parasitic elements at (a) 2.0 and (b) 2.6 GHz.

2.3. Parameters Study

To investigate the design guidelines of the antenna, the key parameters affecting the impedance bandwidth and 3-dB bandwidth are studied in this section. Other parameters should be kept constant when one parameter is analyzed. Here, the length of each section of the stepped dipole, parasitic loop patches and parasitic strips play important roles in ARBW performance improving. Fig. 5(a) depicts the $|S_{11}|$ and AR curves under different values of d_l1 and d_l2 (the sum of d_l1 and d_l2 is kept to a constant). The AR minimum at the higher frequency tends to become higher as d_l1 decreases. Meanwhile, the maximum of AR curve at low band rises when d_l1 is changed to 14.5 mm or 13.5 mm. At last, $d\_l1 = 13.5$ mm and $d\_l2 = 16.5$ mm are selected to achieve a wider 3-dB ARBW performance within the operating band. Fig. 5(b) illustrates effects of the length p_l1 on the AR curve. As p_l1 changes, the maximums in low band and high band rise. In addition, the length of p_l1 affects the smoothness of the axis ratio curve. To get a smooth AR curve, $p\_l1 = 25$ mm is selected. Effects of varying the length p_l3 are shown in Fig. 5(c). It can be seen that the curve goes down gradually when p_l3 increases. Moreover, the length of p_l3 also affects the overall resonant frequency band of the antenna. To get a reliable antenna structure and an improved performance, $p\_l3 = 130$ mm is adopted. All the variation has little effect on 10-dB impendence bandwidth in the operating band, mainly due to the impedance matching effects of feeding network.

3. EXPERIMENTAL RESULTS

In order to verify the correctness of the simulation results, the proposed antenna is fabricated and measured. The measured results are in good agreement with the simulated ones, while slight differences are caused by test error and fabrication tolerance. It can be seen from Fig. 6 that the proposed antenna

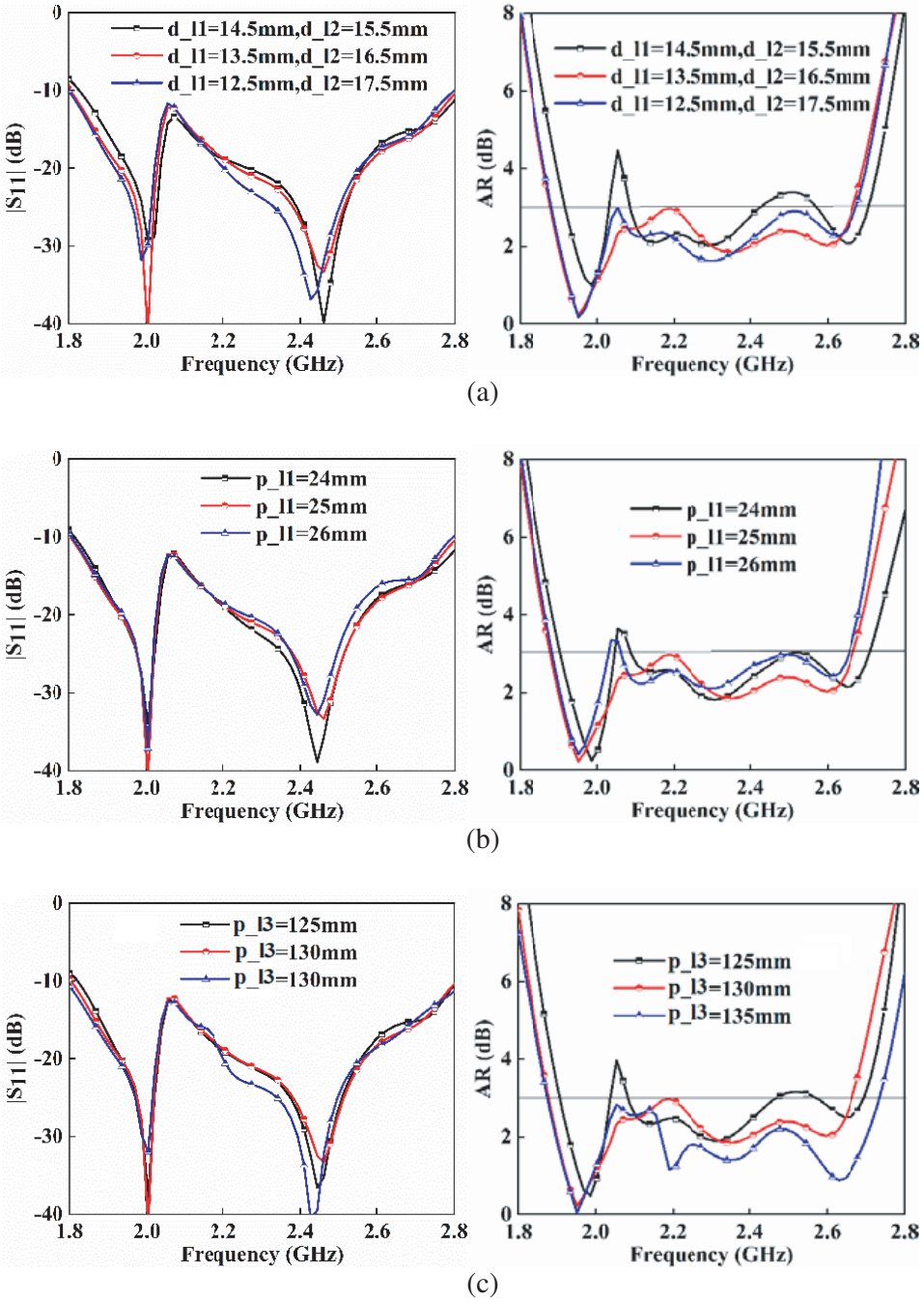

Figure 5. Simulated $|S_{11}|$ and AR pattern for various (a) d_l1 & d_l2; (b) p_l1; (c) p_l3.

achieves an impedance bandwidth of 42% from 1.82 to 2.8 GHz for VSWR $<$ 2 within a 3 dB AR bandwidth of 36.4% from 1.89 to 2.73 GHz. A gain of 9.5 ± 1.5 dBi can be obtained in operating band. The simulated and measured radiation patterns for x-z plane and y-z plane at 2.1 GHz and 2.6 GHz are plotted in Fig. 7, respectively. Several wideband CP antennas are summarized in Table 1, in which λ is the free-space wavelength at the center frequency of the CP antenna. Compared with the reported antennas, this design obtains a wider 3 dB AR bandwidth than that in [12–16] and a lower profile than that in [16–18].

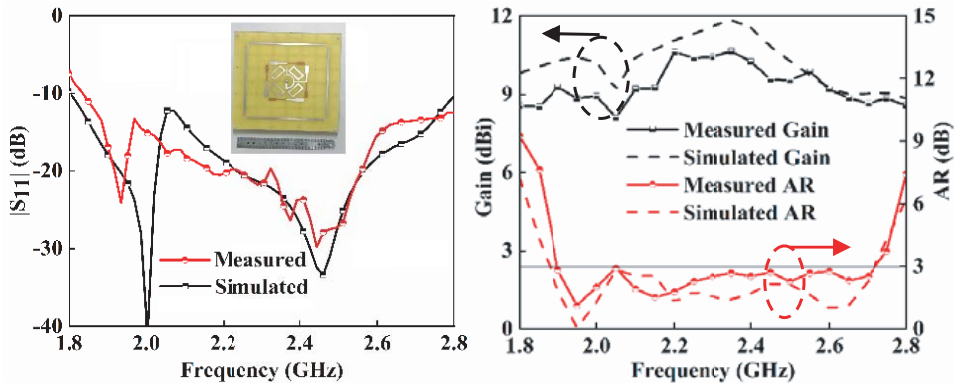

Figure 6. The fabricated prototype of the proposed CP antenna. (a) Simulated and measured $|S_{11}|$, (b) AR and gain characteristics of the proposed antenna.

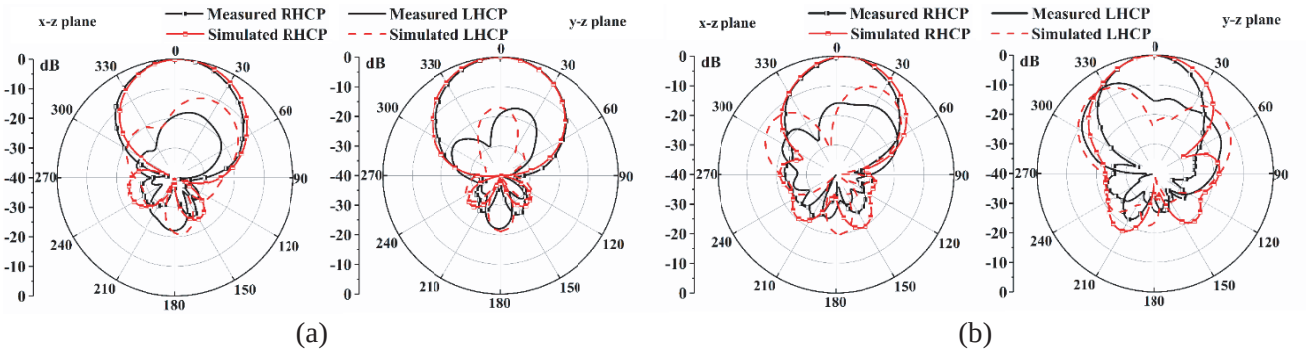

Figure 7. Simulated and measured radiation patterns for x-z and y-z-plane at (a) 2.1 GHz and (b) 2.6 GHz.

Table 1. Summary of several wideband CP antennas.

Ref.	Size (λ^3)	Impedance bandwidth	AR bandwidth	Gain (dBi)	Mat.
12	$0.58 \times 0.58 \times 0.11$	44.5%	27.5%	~ 7.2	HIS
16	$0.97 \times 0.97 \times 0.25$	60.5%	31.0%	8.1 ± 0.2	N/A
18	$0.70 \times 0.70 \times 0.25$	66.2%	41.3%	6	N/A
Pro.	$1.38 \times 1.38 \times 0.13$	37.1%	35.0%	9.5 ± 1.5	AMC

4. CONCLUSION

In this letter, a broadband low-profile circularly polarized antenna with an artificial magnetic conductor (AMC) reflector is proposed. The principle of the circularly polarized antenna is analyzed. Parasitic elements are loaded to improve the circular polarization performance of the antenna. To reduce size of the antenna, an AMC reflector is used, and the proposed antenna obtains a profile of 17 mm (0.125λ) at last. Measured results show that the proposed antenna achieves an impedance bandwidth of 42% from 1.82 to 2.8 GHz for VSWR < 2 within a 3 dB AR bandwidth of 36.4% from 1.89 to 2.73 GHz. The circularly polarized operating band of the proposed antenna includes 3G/4G and WLAN band (1.8 to 2.7 GHz). For its low profile and broadband characteristics, the proposed antenna has broad application prospects in systems that operate from 1.88 to 2.67 GHz.

REFERENCES

1. Ta, S. X., I. Park, and R. W. Ziolkowski, "Circularly polarized crossed dipole on an HIS for 2.4/5.2/5.8-GHz WLAN applications," *IEEE Antennas & Wireless Propagation Letters*, Vol. 12, No. 3, 1464–1467, 2013.
2. Lin, W., et al., "Reconfigurable, wideband, low-profile, circularly polarized antenna and array enabled by an artificial magnetic conductor ground," *IEEE Transactions on Antennas & Propagation*, Vol. 66, No. 3, 1564–1569, 2018.
3. Wu, J., et al., "Broadband circularly polarized patch antenna with parasitic strips," *IEEE Antennas & Wireless Propagation Letters*, Vol. 14, 559–562, 2015.
4. Chang, T.-N. and J.-H. Jiang, "Enhance gain and bandwidth of circularly polarized microstrip patch antenna using gap-coupled method," *Progress In Electromagnetics Research*, Vol. 96, 127–139, 2009.
5. Yang, W., et al., "Single-fed low profile broadband circularly polarized stacked patch antenna," *IEEE Transactions on Antennas & Propagation*, Vol. 62, No. 10, 5406–5410, 2014.
6. Le, T. T., H. H. Tran, and H. C. Park, "Simple-structured dual-slot broadband circularly polarized antenna," *IEEE Antennas & Wireless Propagation Letters*, Vol. 17, No. 3, 476–479, 2018.
7. Gyasi, K. O., et al., "A compact broadband cross-shaped circularly polarized planar monopole antenna with a ground plane extension," *IEEE Antennas & Wireless Propagation Letters*, Vol. 17, No. 2, 335–338, 2018.
8. Wang, C. J. and W. B. Tsai, "Microstrip open-slot antenna with broadband circular polarization and impedance bandwidth," *IEEE Transactions on Antennas & Propagation*, Vol. 64, No. 9, 4095–4098, 2016.
9. Ding, K., Y. X. Guo, and C. Gao, "CPW-fed wideband circularly polarized printed monopole antenna with open loop and asymmetric ground plane," *IEEE Antennas & Wireless Propagation Letters*, Vol. 16, 833–836, 2017.
10. Chen, Z.-F., et al., "A CPW-fed broadband circularly polarized wide slot antenna with modified shape of slot and modified feeding structure," *Microwave & Optical Technology Letters*, Vol. 58, No. 6, 1453–1457, 2016.
11. Ding, K., et al., "Gain-improved broadband circularly polarized antenna array with parasitic patches," *IEEE Antennas & Wireless Propagation Letters*, Vol. 16, 1468–1471, 2017.
12. Lin, S. K. and Y. C. Lin, "A compact sequential-phase feed using uniform transmission lines for circularly polarized sequential-rotation arrays," *IEEE Transactions on Antennas & Propagation*, Vol. 59, No. 7, 2721–2724, 2011.
13. Ta, S. X. and I. Park, "Compact wideband circularly polarized patch antenna array using metasurface," *IEEE Antennas & Wireless Propagation Letters*, Vol. 16, 1932–1936, 2017.
14. Chatterjee, J., A. Mohan, and V. Dixit, "Broadband circularly polarized H-shaped patch antenna using reactive impedance surface," *IEEE Antennas & Wireless Propagation Letters*, Vol. 17, No. 4, 625–628, 2018.
15. Feng, D., et al., "A broadband low-profile circular polarized antenna on an AMC reflector," *IEEE Antennas & Wireless Propagation Letters*, Vol. 16, 2840–2843, 2017.
16. Agarwal, K., Nasimuddin, and A. Alphones, "Wideband circularly polarized AMC reflector backed aperture antenna," *IEEE Transactions on Antennas & Propagation*, Vol. 61, No. 3, 1456–1461, 2013.
17. Tu, Z. H., K. Jia, and Y. Y. Liu, "A differentially fed wideband circularly polarized antenna," *IEEE Antennas & Wireless Propagation Letters*, Vol. 17, No. 5, 861–864, 2018.
18. Xu, R., J. Y. Li, and K. Wei, "A broadband circularly polarized crossed-dipole antenna," *IEEE Transactions on Antennas & Propagation*, Vol. 64, No. 10, 4509–4513, 2016.